Egypt. J. Chem. **Vol. 68**, No.4 pp. 157 - 165 (2025)

Egyptian Journal of Chemistry

http://ejchem.journals.ekb.eg/

Development of a Highly sensitive Methionine Sensor based on Copper Phthalocyanine and Gold Nanoparticles-Modified Carbon Paste Electrode

Hany M. Mohamed[a], Abdellatef A. Radowan[a]*

[a] *Chemistry Department, Faculty of Science, Taif University, Saudi Arabia.*

[b]*Applied Organic Chemistry Department, National Research Centre, El Bohouth St., Dokki, 12622 Giza, Egypt.*

Abstract

A novel electrochemical sensor for the sensitive and selective detection of methionine (Met) has been developed, utilizing copper (II)phthalocyanine (CuPc)-gold nanoparticles (AuNPs)– modified carbon paste electrode (CPE). This sensor was thoroughly characterized using a combination of techniques including cyclic voltammetry (CV), and electrochemical impedance spectroscopy (EIS). Cyclic voltammetry studies revealed a significant enhancement in the electrochemical behavior of methionine at the CuPc–AuNPs modified carbon paste electrode (CuPc-AuNPs/CPE) compared to both the unmodified carbon paste electrode and modified CuPc-CPE. The increase of the anodic redox signal for methionine was credited to a catalytic effect of AuNPs. This effect was examined using three different CPEs with varying concentrations of Au nanoparticles (0.03, 0.06, and 0.12 wt.%), while each electrode contained a fixed amount of CuPc (0.6 wt%). The sensor fabricated with 0.06% AuNPs exhibited superior sensitivity, as evidenced by differential pulse voltammetry analysis. This sensor exhibited an analytical range of 2.0 –150 µM and a limit of detection (LOD) of 0.5 µM. The developed sensor was successfully applied for the determination of methionine in pharmaceutical preparations.

Keywords: Methionine; phthalocyanine; electrochemical sensor; gold nanoparticles; cyclic voltammetry; differential pulse voltammetry.

1. Introduction

Methionine, (2-amino-4-(methylthio) butanoic acid) the structure is shown in (figure 1), an essential amino acid, plays a crucial role in various physiological functions, including protein synthesis, methylation, sulfur metabolism, and immune responses [1]. However, maintaining appropriate methionine levels is critical for health, as deficiencies or excesses can lead to a range of issues [2]. Methionine deficiency can impact growth, particularly in children, and may contribute to muscle weakness, fatty liver disease, mood disorders, cognitive impairment, and nerve problems [3, 4]. Conversely, high methionine levels have been linked to increased homocysteine levels, a risk factor for cardiovascular disease and stroke [5], as well as cognitive decline and an elevated risk of Alzheimer's disease [6, 7]. Excessive methionine intake during pregnancy can also negatively affect fetal development [8, 9]. These health implications underscore the importance of accurately measuring methionine concentrations in biological samples, food, and pharmaceutical preparations [10-12].

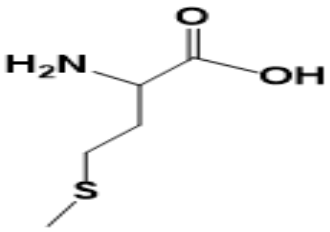

Fig. 1. Chemical Structure for Methionine Compound.

*Corresponding author e-mail: celotfy@yahoo.com.(Abdellatef A. Radowan)
Receive Date: 23 July 2024, Revise Date: 13 August 2024, Accept Date: 28 August 2024
DOI: 10.21608/ejchem.2024.306703.10070

While traditional methods like HPLC [13], chemiluminescence [14], and fluorescence microscopy have been used for analysis of methionine [15], these methods often require complex instrumentation, expensive reagents, and extensive sample preparation. Electrochemical sensors offer a more convenient and cost-effective alternative due to their high sensitivity, rapid response, and suitability for on-site analysis [16]. However, unmodified carbon electrodes exhibit limited sensitivity and selectivity for methionine detection [17].

Recent advancements in electrochemical sensing have focused on the development of sensors utilizing novel nanomaterials and mediators to enhance sensitivity and stability [18]. Gold nanoparticles (AuNPs) have emerged as particularly promising materials in this field, owing to their unique combination of advantageous properties such as extensive high conductivity, large surface area, biocompatibility, and electro-catalytic properties [19]. Metallo-phthalocyanines (MPcs), synthetic porphyrin analogues with a central metal atom, have also emerged as promising electrochemical mediators [20]. These compounds exhibit exceptional electronic properties, rendering them highly suitable for applications in various fields, including biosensors [21, 22]. This work presents the design of a novel electrochemical sensor for methionine with highly sensitive and selective detection. Our sensor is based on a carbon paste electrode modified with a synergistic combination of AuNPs and Copper (II) phthalocyanine (CuPc). The synergistic effect of AuNPs and CuPc enhances the electrochemical response of methionine, leading to a significant improvement in sensitivity compared to unmodified or CuPc-only modified carbon paste electrodes.

2 Experimental

2.1 Materials and Methods

Graphite powder (<150 μm, with high purity) and paraffin oil were purchased from Riedel-de Haën. Phthalic anhydride was obtained from Fluka. Tetrachloroauric(III) acid trihydrate ($HAuCl_4.3H_2O$), anhydrous copper(II) chloride (99.99%), and methionine were procured from BDH and Reanal, respectively. Britton-Robinson (BR) buffer solution (4.0×10^{-2} mol L^{-1}) was used as the supporting electrolyte.

2.2 Synthesis of Cu (II) Phthalocyanine (CuPc)

Cu(II)Pc was synthesized using a modified method for the synthesis of metallophthalocyanines (MPcs)[23]. Briefly, the reaction mixture was prepared by adding 5.925 g phthalic anhydride (0.04 mol), 1.34 g Copper (II) chloride anhydrous (0.01 mol), excess urea (25 g), and a trace amount of ammonium molybdate tetrahydrate catalyst (0.01 g) to a round-bottom flask containing 30 mL of nitrobenzene. The reaction mixture was refluxed at 200 °C with continuous stirring for about 5.0 hours, until a dark blue color indicated the completion of the reaction. After cooling, the reaction mixture was then filtered and washed repeatedly with 1.0 M HCl and 1.0 M NaOH until a colorless filtrate was obtained in each case. This washing process ensured the removal of any unreacted starting materials or byproducts. The synthesized copper (II) phthalocyanine catalyst was labelled as CuPc**.**

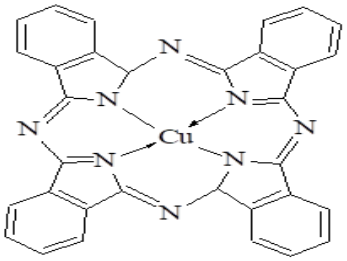

Fig. 2. Structure of Copper (II) phthalocyanine (CuPc).

2.3 Synthesis of Gold Nanoparticles (AuNPs)

To prepare a 0.01% (w/v) solution of $HAuCl_4.3H_2O$, by dissolving 0.01 g of the salt in 100.0 mL of distilled water. Then boil the solution and add 2.0 mL of 1.0% (w/v) of trisodium citrate solution rapidly under vigorous stirring [22]. The color was changed from pale yellow color to blue, and finally to red color, indicating formation of AuNPs. The solution of reaction was then allowed for cooling to room temperature and stored at 4°C. The prepared AuNP stock solution had a concentration of 50.0 mg/L.

2.4 Preparation of CuPc-Modified Carbon Paste (CuPc–CP) and CuPc–AuNP Modified Carbon Paste (CuPc–AuNP/CP)

Bare carbon pastes (CPs) were prepared by mixing 0.20 g of graphite powder with 0.80 g of paraffin oil in a ceramic mortar for 15 minutes. The resulting homogeneous paste was packed into Teflon piston holders, each with a 5 mm radius active surface area [19]. Conductive electric screws were used to ensure electrical contact with the potentiostat. The surface of electrode was regenerated by polishing with wet filter paper to obtain on smooth and a shiny surface [24].

To fabricate CuPc–CP electrodes, 10.0 µL of a CuPc suspension (1%, 3%, 6%, or 9% in water) was drop-cast onto the surface of bare carbon paste electrodes (CPEs) three times, allowing each layer to dry at 25 °C. The modified CPEs were rinsed with double-distilled water before being used in the electrochemical cell. CuPc–AuNP/CP electrodes were prepared using a similar method, where the CuPc catalyst was mixed with AuNPs (0%, 0.03%, 0.06%, or 0.12%). Table 1 provides a detailed breakdown of the compositions of all electrodes, including the CP bare electrode.

Table 1: Compositions of the Different Carbon Paste Electrodes and Rct Values

Ele #	Graphite (g)	CuPc (%)	Paraffin (g)	AuNPs (%)	R_{ct} (Ω)
1	0.2	0	0.8	0	700
2	0.2	0.1	0.8	0	350
3	0.2	0.3	0.8	0	265
4	0.2	0.6	0.8	0	200
5	0.2	0.9	0.8	0	210
6	0.2	0.6	0.8	0.03	140
7	0.2	0.6	0.8	0.06	130
8	0.2	0.6	0.8	0.12	129
9	0.2	0	0.8	0.06	320

2.5 Electrode Fabrication and Characterization

Shimadzu spectrophotometer model (UV-2401) is used to record UV-visible spectra. electrochemical workstation from CH Instruments Inc. model (CHI 660D) is used for electrochemical measurements, including CV, EIS, and DPV. A three-electrode system was employed for electrochemical measurements, consisting of a working carbon paste electrode, a double junction silver/silver chloride (Ag/AgCl) reference electrode, and a platinum wire counter electrode**.**

3. Results and Discussion

3.1 Electrochemical Characterization

The electrochemical properties of the carbon paste electrodes were investigated using cyclic voltammetry. The electrodes were immersed in a $5.0X10^{-3}$ M $[Fe(CN)_6]^{3-/4-}$ in 0.1 M KCl solution and scanned through a window of potential is between 0.0 V to 1.0 V with a scan rate of 0.1 V s^{-1}. The cyclic voltammogram of the unmodified carbon paste electrode (CP) (Table1, electrode #1) exhibited characteristic peaks of oxidation and reduction was related to the transfer of electron process between the electrode and the $[Fe(CN)_6]^{3-/4-}$ solution. The potential peak (Ep) for this redox process was observed at 571 mV. The addition of AuNPs with the carbon paste significantly enhanced both the oxidation and reduction peak currents. Furthermore, the addition of AuNPs resulted in a shift of the oxidation peak to a more negative potential and the reduction peak to a more positive potential (Ep = 496 mV), compared to the unmodified CP electrode. This enhancement in peak currents, coupled with the shift in peak potentials, evidenced (Table1, electrode #9) the benefit of AuNPs in improving the conductivity and overall electrochemical characteristics of the carbon paste.

Further the process of electron transfer enhancement was observed upon the presence of CuPc on the carbon paste (Ep = 428 mV for CuPc–CP, Table1, electrode #4). The addition of CuPc to the AuNP-modified carbon paste (Ep = 431 mV for CuPc–AuNP/CP, Table1, electrode #7) resulted in a significant enhancement of the oxidation and reduction processes. This was manifested by the redox couple oxidizing at a more negative potential and reducing at a more positive potential, indicating an improvement in electron transfer kinetics. This observation confirmed the positive impact of AuNPs on the process of electron transfer within the carbon paste, highlighting their ability to enhance electrochemical performance. The CuPc-CP electrode exhibited improved transfer of electron characteristics compared to the unmodified CPE, due to the mediating properties of the addition of CuPc. The simultaneous addition of both AuNPs and CuPc to the carbon paste (CuPc–AuNP/CP) led to a further enhancement of the characteristic's electron transfer. This enhanced response observed for the CuPc–AuNP/CP electrode is related to the synergistic combination of the AuNPs' improved conductivity and the catalytic potential of the CuPc mediator. It is well-established that dispersed AuNPs can significantly enhance catalytic activity within bimetallic systems. These improvements in electrochemical characteristics are further investigated and discussed in detail within the EIS studies.

3.2 Electrochemical Impedance Spectroscopy (EIS)

Electrochemical impedance spectroscopy (EIS) was employed to probe the charge transfer kinetics at the electrode interface. Using the $[Fe(CN)_6]^{3-/4-}$ redox couple as a probe, Nyquist plots were obtained for various CP electrodes in the frequency range of 0.1 Hz to 10^5 Hz at a potential of 0.43 V (Figure 7). The semicircle diameter, corresponding to charge transfer resistance (R_{ct}), was used to assess the interfacial properties of the electrodes. The spectra of impedance obtained exhibits a semicircle portion at higher frequencies, relating to the electron transfer-limited process, and a linear portion at lower frequencies, showing the process of diffusion-limited.

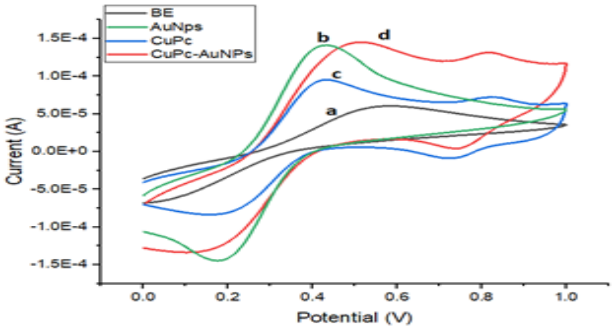

Fig. 3. Cyclic voltammograms of the following electrodes in $5.0X10^{-3}$ M $[Fe(CN)_6]^{3-/4-}$ in 0.1 M KCl solution: (a) unmodified carbon paste electrode (CP), (b) AuNP-modified carbon paste electrode (AuNP/CP), (c) CuPc-modified carbon paste electrode (CuPc–CP), and (d) CuPc–AuNP-modified carbon paste electrode (CuPc–AuNP/CP).

The diameter of the semicircle in the impedance spectrum is a direct measure of the resistance of charge transfer (R_{ct}), which governs the electron-transfer kinetics of the redox couple at the interface of electrode. Hence, R_{ct} serves as a valuable parameter for characterizing the interfacial properties of the electrode, providing insights into the efficiency of electron transfer at the electrode-electrolyte interface. As depicted in Figure 7, The carbon paste electrode (CPE) exhibited a considerable resistance to the process of electron transfer, as evidenced by a large semicircle domain in the Nyquist plot, corresponding to a charge transfer resistance (R_{ct}) of 700 Ω. The addition of AuNPs to the CPE resulted in a notable decrease in resistance, with a reduced charge transfer resistance (R_{ct}) of 320 Ω. Added CuPc modifier (6%) to the CPE resulted in a smaller semicircle domain, indicating a lower resistance for the electron-transfer of the redox couple (R_{ct} = 140 Ω). This reduction in resistance is likely attributed to the presence of the CuPc mediator, which facilitates electron transfer. The further of AuNPs addition to the CuPc-CP (CuPc–AuNP/CP, 0.06%) significantly decreased the R_{ct} value to 130 Ω, demonstrating a substantial improvement in electron transfer kinetics. This substantial decrease in charge transfer resistance highlights the significant impact of AuNPs on the process of electron transfer, indicating their crucial function in enhancing the electrochemical efficiency of the modified electrode.

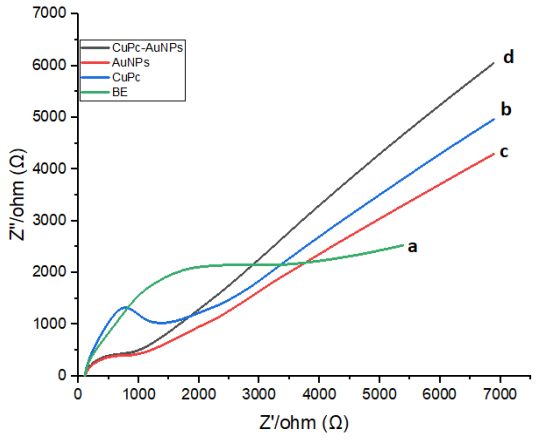

Fig. 4: Comparison of EIS responses for different carbon paste electrodes: (a) unmodified carbon paste electrode (CP), (b) CuPc-modified carbon paste electrode (CuPc/CP), (c) AuNPs-modified carbon paste electrode (AuNPs/CP), and (d) CuPc-AuNPs-modified carbon paste electrode (CuPc-AuNPs/CP

.

3.3 Optimization of CuPc and AuNP Concentrations

To further optimize the characteristics of the carbon paste, a systematic investigation was conducted to evaluate the impact of varying concentrations of CuPc and AuNPs. The optimal percentage of CuPc modifier was determined through a series of EIS studies, aiming to identify the concentration that yielded the most favorable electrochemical characteristics. As observed in Figure 4 and Table 1, increasing the CuPc modifier percentage resulted in a decrease in paste resistance (R_{ct}) up to 0.6% CuPc (from 0.1% to 0.6%, electrodes 2-4 in Table 1). This trend is attributed to the catalytic activity of CuPc, which facilitates electron transfer and lowers the resistance. However, further increasing the CuPc percentage beyond 0.6% led to an increase in resistance (0.9%, electrode #5, Table 1). This suggests that at higher concentrations, the paste might become hindered by the excess modifier, impeding the electron transfer process. Therefore, to optimize the sensor's performance, 0.6% CuPc was selected as the optimal modifier for further studies, as it demonstrated the most efficient electron transfer characteristics, evidenced by the minimized charge transfer resistance.

Three electrodes, each containing 0.6% CuPc but varying AuNP percentages (electrodes #6-8 in Table 1), were fabricated and evaluated to determine the optimal AuNP concentration. The electrode containing 0.06% AuNPs and 0.6% CuPc (electrode #7) exhibited lower resistance compared to the electrode containing 0.03% AuNPs and 0.6% CuPc (electrode #6). This confirmed that increasing the amount of AuNPs to CPE resulted in a decrease in resistance, suggesting a direct correlation between AuNP concentration and improved electron transfer kinetics. Despite further increases in AuNP content beyond 0.06%, no significant additional decrease in electron transfer resistance (R_{ct}) was observed, indicating that an optimal concentration had been reached. This suggests that, at higher concentrations, AuNP agglomeration might occur within the paste, hindering their beneficial effects on conductivity. Therefore, the electrode labeled 7, containing 0.06% AuNPs and 0.6% CuPc, emerged as the most promising option for further studies based on its optimized electrochemical performance. Based on the comprehensive investigations presented in Figure 4 and Table 1, This optimized electrode was chosen as the foundation for a voltammetric sensor designed to detect methionine. The synergistic effect of the AuNPs, enhancing conductivity, and the CuPc redox mediator, facilitating electron transfer, collectively facilitated the oxidation of methionine at the electrode surface. Table 1 offers a comprehensive summary of the compositions of the electrodes at different stages of modification, along with their corresponding charge transfer resistance (R_{ct}) values, which are critical parameters for evaluating the efficiency of electron transfer at the electrode interface.

3.4 Electrochemical Behavior of Methionine at Different pH Values

Cyclic voltammograms recorded for methionine oxidation demonstrated a gradual improvement in peak current response with increasing pH, reaching optimal performance at pH 5.0. At higher pH levels beyond 5.0, the methionine oxidation peaks decreased, reaching their lowest point at pH 11.0 (Figure 8a). The oxidation peak potentials exhibited a shift towards more negative values as the pH increased, closely following Nernstian behavior (Ep(V) = 0.88953 - 0.06672 [pH], r=-0.98754), as illustrated in Figure 8b. This linear relationship between the oxidation peak potential and pH, closely following Nernstian behavior, indicates the involvement of an equal number of protons and electrons in the oxidation of methionine at the electrode surface. This observation highlights the critical role of protons in the methionine oxidation process. The low value of the intercept in the Nernstian equation suggests a single, dominant reaction mechanism for methionine oxidation, with minimal contributions from side reactions.

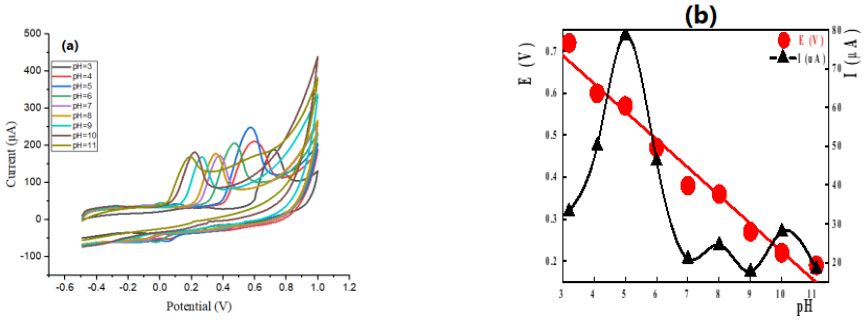

Fig. 5: (a) Cyclic voltammograms at different pH values; b) pH effect on the (Met) peak current and potential. CuPc-AuNPs/CPEs for 30.0 ng mL^{-1} methionine in BR buffer. Scan rate was 50 mV s^{-1}.

4. Electro-analytical Studies

4.1 Electrochemical Evaluation of Methionine

To evaluate the sensor's response to methionine, cyclic voltammetry was employed with various carbon paste electrodes: unmodified (CP), AuNP-modified (AuNP/CP), CuPc-modified (CuPc–CP), and the combined AuNP-CuPc modified (CuPc–

AuNP/CP) electrodes. The electrochemical experiments were conducted in a Britton-Robinson (BR) buffer solution at pH 5, using a methionine concentration of 30.0 ng mL^{-1}. The potential was swept linearly from 0.0 V to 1.0 V at a scan rate of 0.05 V s^{-1}. The results demonstrated a significant enhancement in the methionine oxidation current for both AuNP/CP and CuPc–CP electrodes compared to the unmodified CP electrode. This highlights the positive impact of these modifications in improving the electrode's sensitivity towards methionine oxidation. Notably, the cathodic shift in the peak potential observed in the presence of methionine further emphasized This observation further underscores the crucial role of AuNPs in enhancing the electrode's overall performance, particularly in facilitating methionine oxidation.

4.2 Investigating the Impact of Scan Rate

The influence of scan rate on the electrochemical behavior of methionine was investigated through cyclic voltammetry experiments. By systematically varying the scan rate from 0.025 to 0.150 Vs^{-1}, we observed a consistent shift in the peak potential towards more positive values as the scan rate increased, accompanied by a corresponding increase in the peak current[25, 26]. This observation suggested an irreversible oxidation process for methionine at the electrode surface. The linear correlation between the peak current and the square root of the scan rate (r=0.99344), as depicted in Figure 6b, further confirms the irreversible nature of the methionine oxidation reaction at the electrode surface. Additionally, the linear relationship between the logarithmic values of the peak current and the scan rate, with a slope of 0.99603 (Figure 6c), suggests that the methionine oxidation process is predominantly controlled by an adsorption-controlled reaction mechanism.

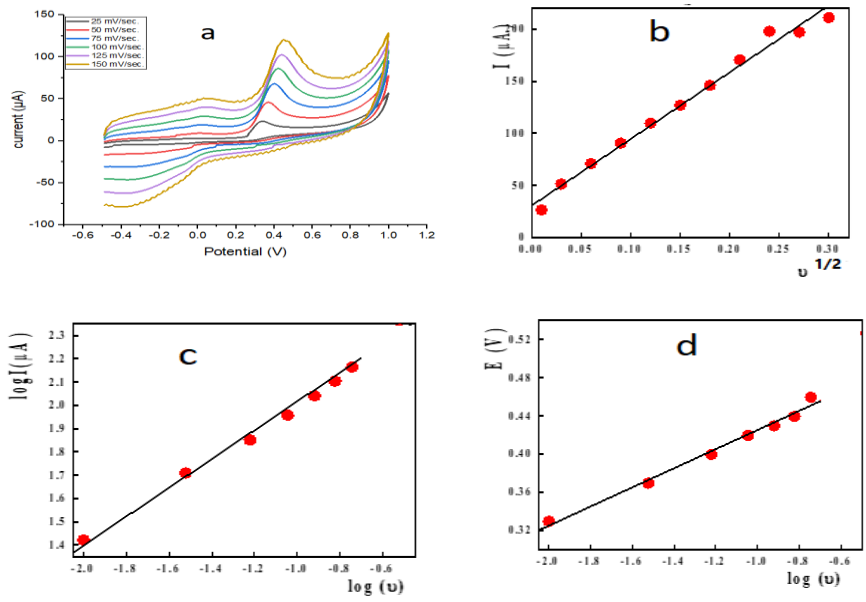

Fig. 6. Voltammetric behavior of 30.0 ng mL^{-1} methionine (Met) recorded at the CuPc-AuNPs/CPE electrode in Britton-Robinson (BR) buffer solution at pH 5, applying different sweep rates: (a) cyclic voltammograms at various scan rates, (b) plot of current peak (Ip) vs. square root of scan rate (υ1/2), (c) plot of log (Ip) vs. log (υ), and (d) plot of peak potential (Ep) vs. log (υ).

Furthermore, the peak potential displayed a linear dependence on the logarithmic value of the sweep rate (Figure 9d, EP(V) = 0.52547 + 0.10022 [log υ (Vs^{-1})], r=0.99478). This linear relationship provides valuable insights into the kinetics of the electrochemical process, suggesting that the oxidation reaction is governed by a mixed-controlled process involving both charge transfer and diffusion limitations[27].

4.3 Establishing the Sensor's Analytical Range and Sensitivity

To determine the sensor's analytical range and sensitivity, a series of differential pulse voltammetry (DPV) experiments were performed with varying concentrations of methionine in BR buffer (pH 5) at a potential of 0.55 V. The resulting data was analyzed to construct a calibration curve (Figure 7b), which showed a linear relationship (R^2 = 0.9894) between the methionine oxidation current and its concentration within the range of 2.0–150 µM. The sensor exhibited a sensitivity of

12.35 µA mM^{-1} (58.9 µA mM^{-1} cm^{-2}) and a limit of detection (LOD) of 0.50 µM. The %RSD value for the sensor was 6.8%, demonstrating good repeatability. Further analysis of the repeatability using five fresh electrodes with the same optimized composition at a concentration of 100 µM methionine resulted in a %RSD of 8.7%, confirming the robust performance and reliability of the CuPc–AuNP/CP electrode.

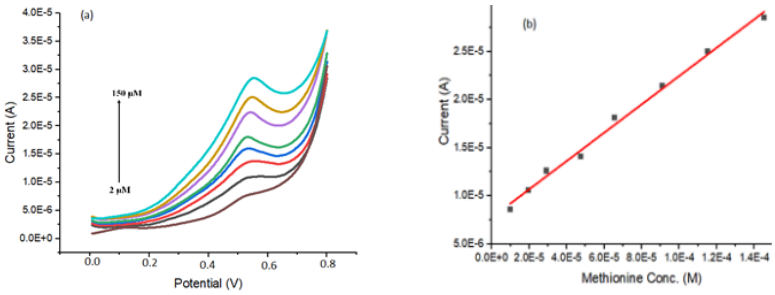

Fig. 7. (a) Differential pulse voltammetry (DPV) response of the AuNP-CuPc-modified carbon paste electrode (AuNP–CuPc–CP) at different concentrations of methionine (2–150 µM) in Britton-Robinson (BR) buffer (pH 5) at a potential of 0.55 V. (b) Calibration curve showing the relationship between the peak current and the concentration of methionine obtained from the DPV response of the CuPc–AuNP/CP electrode.

5. Interference and Real-World Application Studies

To evaluate the sensor's selectivity and practical applicability, interference studies were conducted in the presence of common potential interferents, including ascorbic acid (vitamin C), glutathione, and L-cysteine. These analytes were chosen due to their presence in biological samples and their potential to interfere with methionine detection. The percentage recovery of methionine was measured by introducing increasing concentrations of the interferents (up to 3-fold of the methionine concentration) and observing the resulting change in the methionine oxidation current. The results, summarized in Table 2, showed a significant interference from ascorbic acid, with a recovery of only 33.5% at a 3-fold excess. However, glutathione and L-cysteine exhibited minimal interference, with recovery values exceeding 90% even at a 3-fold excess.

Table 2: Interference response data for CuPc–AuNP/CP

	Recovery (%)		
Interferent	1 : 1	1 : 2	**1 : 3**
Ascorbic acid	59.5	48.3	**33.5**
Glutathione	98.3	95.2	**91.5**
cysteine	**95.3**	**90.6**	**88.6**

To demonstrate the sensor's practical utility, it was used to determine methionine concentrations in pharmaceutical capsules (Solgar Co.) and a dietary supplement (glutathione enhancer, Marcyrl Co.). The results, presented in Table 3, showed good agreement between the expected and measured methionine concentrations, with recovery values exceeding 97%. These findings highlighted the sensor's potential for real-world applications in pharmaceutical and food analysis.

Table 3: Methionine Determination in Pharmaceutical Samples

Sample	**Added (ppm)**	**Found (ppm)**	**Recovery (%)**
L-Methionine 500	100.0	98.8	98.8 (± 3.5)
glutathione enhancer	100.0	97.9	97.9 (± 2.9)

6. Conclusions

This research successfully developed a highly sensitive electrochemical sensor for methionine detection, utilizing a carbon paste electrode modified with gold nanoparticles and copper (II) phthalocyanine. The developed sensor demonstrated excellent performance characteristics, including a wide linear range of 2.0–150 µM, a low limit of detection of 0.50 µM, and

good repeatability. The inclusion of AuNPs significantly enhanced the electrode's electron transfer characteristics, while the catalytic properties of CuPc contributed to the sensor's high sensitivity.

The sensor demonstrated satisfactory selectivity against common interferents, indicating its potential for practical applications in pharmaceutical and food analysis. These findings highlight the significant promise of electrochemical sensors in providing a convenient, cost-effective, and sensitive approach for the accurate determination of methionine in various matrices, opening up possibilities for wider applications in diverse fields.

7. Conflicts of interest

The authors declare that they have no known competing financial interests or personal relationships that could have appeared to influence the work reported in this paper.

8. References

1. Wang L, Gao C, Wang B, Wang C, Sagada G, Yan Y: Methionine in fish health and nutrition: Potential mechanisms, affecting factors, and future perspectives. *Aquaculture* 2023, 568:739310.
2. Jiang Y, Mistretta B, Elsea S, Sun Q: Simultaneous determination of plasma total homocysteine and methionine by liquid chromatography-tandem mass spectrometry. *Clinica Chimica Acta* 2017, 464:93-97.
3. Aroucha RJN, Ribeiro FB, Bomfim MAD, de Siqueira JC, Marchão RS, Nascimento DCNd: Digestible methionine plus cystine requirement in tambaqui (Colossoma macropomum) diets: Growth performance and plasma biochemistry. *Aquaculture Reports* 2023, 32:101725.
4. Liu Y, Chen W, Zhang S, Zhu X, Wu H, Meng Q, Khan MZ, Yu Z, Zhou Z: N-acetyl-l-methionine dietary supplementation improves meat quality by oxidative stability of finishing Angus heifers. *Meat Science* 2024, 214:109499.
5. Garlick PJ: Toxicity of Methionine in Humans1. *The Journal of Nutrition* 2006, 136(6):1722S-1725S.
6. Alachkar A, Agrawal S, Baboldashtian M, Nuseir K, Salazar J, Agrawal A: L-methionine enhances neuroinflammation and impairs neurogenesis: Implication for Alzheimer's disease. *Journal of Neuroimmunology* 2022, 366:577843.
7. Arumugasamy SK, Chellasamy G, Gopi S, Govindaraju S, Yun K: Current advances in the detection of neurotransmitters by nanomaterials: An update. *TrAC Trends in Analytical Chemistry* 2020, 123:115766.
8. McCarthy N, Weaver AC, Agenbag B, Flinn T, Brougham B-J, Swinbourne AM, Kelly JM, Kleemann DO, Gatford KL, van Wettere WHEJ: Maternal lysine, methionine and choline supplementation in twin-bearing Merino ewes during mid-to-late gestation does not alter pregnancy outcomes or progeny growth and survival. *Livestock Science* 2021, 251:104620.
9. Hargrove DM, Rogers QR, Calvert CC, Morris JG: Effects of Dietary Excesses of the Branched-Chain Amino Acids on Growth, Food Intake and Plasma Amino Acid Concentrations of Kittens. *The Journal of Nutrition* 1988, 118(3):311-320.
10. Günsel A, Kobyaoğlu A, Bilgiçli AT, Tüzün B, Tosun B, Arabaci G, Yarasir MN: Novel biologically active metallophthalocyanines as promising antioxidant-antibacterial agents: Synthesis, characterization and computational properties. *Journal of Molecular Structure* 2020, 1200:127127.
11. Şaylan M, Er EÖ, Tekin Z, Bakırdere S: An accurate and sensitive analytical method for the simultaneous determination of glycine, methionine and homocysteine in biological matrices by matrix matching strategy and LC–quadrupole-time-of-flight-MS/MS. *Spectrochimica Acta Part A: Molecular and Biomolecular Spectroscopy* 2020, 239:118394.
12. Wu S, Lan X, Huang F, Luo Z, Ju H, Meng C, Duan C: Selective electrochemical detection of cysteine in complex serum by graphene nanoribbon. *Biosensors and Bioelectronics* 2012, 32(1):293-296.
13. Baxter JH, Lai C-S, Phillips RR, Dowlati L, Chio JJ, Luebbers ST, Dimler SR, Johns PW: Direct determination of methionine sulfoxide in milk proteins by enzyme hydrolysis/high-performance liquid chromatography. *Journal of Chromatography A* 2007, 1157(1):10-16.
14. Yang Y, Han S: Synergistic enhanced of carbon dots and eosin Y on fenton chemiluminescence for the determination of methionine. *Microchemical Journal* 2021, 163:105902.
15. Liu J, Ma W, Wang Y, Gu Q, Pan Q, Zong S, Qin M, Li J: Enhanced oxidase-mimic constructed by luminescent carbon dots loaded on MIL-53(Fe)-NO2 for dual-mode detection of gallic acid and biothiols in food and humans. *Food Chemistry* 2024, 433:137241.
16. Akbari Hasanjani HR, Zarei K: An electrochemical sensor for attomolar determination of mercury(II) using DNA/poly-L-methionine-gold nanoparticles/pencil graphite electrode. *Biosensors and Bioelectronics* 2019, 128:1-8.
17. Aslan M, Aydın F, Levent A: Voltammetric studies and spectroscopic investigations of the interaction of an anticancer drug bevacizumab-DNA and analytical applications of disposable pencil graphite sensor. *Talanta* 2023, 265:124893.
18. Gupta S, Tai N-H: Carbon nanomaterials and their composites for electrochemical glucose biosensors: A review on fabrication and sensing properties. *Journal of the Taiwan Institute of Chemical Engineers* 2024, 154:104957.

19. Hendawy HA, Khaled E, Radowan A: Voltammetric Determination of Marbofloxacin at Carbon Paste Sensor Integrated with Copper Oxide Nanoparticles. *Electroanalysis* 2023, 35(5):e202200402.
20. Karaca H, Delibaş NÇ, Sağlam S, Pişkin H, Sezer S, Hökelek T, Teker M: Metallophthalocyanines derived with phenyl sulfide by bridging triazole using click chemistry: Synthesis, Computational Study, Redox Chemistry and Catalytic Activity. *Journal of Molecular Structure* 2021, 1236:130225.
21. Abbas MN, Radwan ALA, B¨¹hlmann P, Ghaffar MAAE: Solid-Contact Perchlorate Sensor with Nanomolar Detection Limit Based on Cobalt Phthalocyanine Ionophores Covalently Attached to Polyacrylamide. *American Journal of Analytical Chemistry* 2011, Vol.02No.07:12.
22. Abbas MN, Saeed AA, Singh B, Radowan AAA, Dempsey E: A cysteine sensor based on a gold nanoparticle–iron phthalocyanine modified graphite paste electrode. *Analytical Methods* 2015, 7:2529-2536.
23. Abbas MN, Radwan ALA, Nooredeen NM, El-Ghaffar MAA: Selective phosphate sensing using copper monoamino-phthalocyanine functionalized acrylate polymer-based solid-state electrode for FIA of environmental waters. *Journal of Solid State Electrochemistry* 2016, 20:1599-1612.
24. Elgrishi N, Rountree KJ, McCarthy BD, Rountree ES, Eisenhart TT, Dempsey JL: A Practical Beginner's Guide to Cyclic Voltammetry. *Journal of Chemical Education* 2018, 95(2):197-206.
25. Eskiköy Bayraktepe D, İnal EK, Yazan Z: Preparation and characterization of a pencil graphite electrode modified with gold nanoparticles decorated poly (l-methionine) and its use in the simultaneous sensitive electrochemical analysis of ascorbic acid, acetaminophen, chlorpheniramine maleate, and caffeine. *Microchemical Journal* 2021, 171:106812.
26. Esfandiari N, Aliofkhazraei M: Advances in the determination of trace amounts of iron cations through electrochemical methods: A comprehensive review of principles and their limits of detection. *Talanta* 2024, 277:126365.
27. Brinda KN, Yhobu Z, Nagaraju DH, Budagumpi S: 2 - Working principle and sensing mechanism of electrochemical sensors. In *2D Materials-Based Electrochemical Sensors.* Edited by Rout CS: Elsevier; 2023: 9-44.